Original Article

Available online at
www.heca-analitika.com/ljes

Leuser Journal of Environmental Studies

Vol. 4, No. 2, 2026

Assessment of Arsenic and Mercury Contamination in Water and Sediments Around the Jaboi Sabang Geothermal Area Using ICP-OES

Fazri Baziahni [1], Rinaldi Idroes [1,2] and Lelifajri Lelifajri [1,*]

[1] Department of Chemistry, Faculty of Mathematics and Natural Sciences, Universitas Syiah Kuala, Banda Aceh 23111, Indonesia; fazribz22@mhs.usk.ac.id (F.B.); rinaldi.idroes@usk.ac.id (R.I.); lelifajri@usk.ac.id (L.L.)
[2] Department of Pharmacy, Faculty of Mathematics and Natural Sciences, Universitas Syiah Kuala, Banda Aceh 23111, Indonesia

* Correspondence: rinaldi.idroes@usk.ac.id

Article History

Received 11 June 2026
Revised 30 September 2026
Accepted 14 October 2026
Available Online 31 October 2026

Keywords:
Geothermal manifestation
Heavy metal contamination
Inductively Coupled Plasma
Environmental monitoring
Water and sediment analysis

Abstract

The Jaboi Sabang Geothermal Area in Aceh, Indonesia, comprises four active craters that release geothermal fluids and gases into surrounding water sources used by local communities for daily activities. Despite the known toxicity of arsenic (As) and mercury (Hg) in geothermal environments, baseline data on their occurrence and distribution in local water and sediment remain limited. This study assessed As and Hg contamination in water and sediment samples using Inductively Coupled Plasma–Optical Emission Spectrometry (ICP-OES). Water samples were collected from hot springs, bathing pools, rivers, boreholes, dug wells, and treated water, while sediment samples were obtained from craters and stream beds. Method validation showed good linearity ($R^2 > 0.99$), with limits of detection (LoD) of 10.49 µg/L for As and 1.98 µg/L for Hg, and acceptable recovery values (70–125%). The highest As and Hg instrument responses in water were observed in hot-spring sample J1, at 11.268 and 6.861 µg/L, respectively. However, the As result for J1 was above the LoD but below the limit of quantification (LoQ), indicating detection without reliable quantification, while As in J2–J7 was below the LoD. For Hg, only J1 exceeded the LoQ, whereas J3 and J6 produced responses between the LoD and LoQ. The remaining samples were below the Hg LoD. Because the applicable Hg benchmark was lower than the method LoD, compliance could not be established for samples other than J1. These findings highlight the need for improved analytical sensitivity and continued monitoring to assess potential environmental and public health risks.

Copyright: © 2026 by the authors. This is an open-access article distributed under the terms of the Creative Commons Attribution-NonCommercial 4.0 International License. (https://creativecommons.org/licenses/by-nc/4.0/)

1. Introduction

Geothermal potential is commonly indicated by the presence of geothermal manifestations occurring at the surface, such as hot springs, fumaroles, mud pools, steaming ground, and altered rocks [1]. Surface geothermal manifestations are generally associated with hydrothermal systems [2]. Beyond their energy potential, geothermal areas naturally release hazardous elements into surrounding environmental media. Among these, arsenic (As) and mercury (Hg) are of particular concern due to their documented toxicity, environmental persistence, and potential to accumulate in water, sediment, and biota [3]. Establishing baseline occurrence and distribution data for these elements in geothermal areas is essential for environmental management and serves as a foundation for subsequent health risk assessments.

Arsenic and mercury are released into the environment through both natural processes, including volcanic and geothermal emissions, and anthropogenic activities [4, 5]. In geothermal systems, arsenic is primarily derived from arsenic-bearing pyrite and arsenopyrite dissolution,

while mercury is released through fumarolic activity and geothermal fluid discharge [4, 5]. Chronic exposure to these elements has been associated with various adverse health effects, including skin lesions, neurological impairment, and kidney dysfunction [6, 7].

While water quality directly influences potential human exposure through consumption and contact, sediment plays an important role as both a sink and a secondary source of potentially toxic elements in aquatic environments. Metals released from geothermal sources can adsorb onto sediment particles, particularly iron oxides, hydroxides, and organic matter, where they may accumulate over time. Changes in environmental conditions, including pH and redox potential, can remobilize sediment-bound metals and release them into the overlying water column, allowing sediment to become a long-term source of contamination [8]. Contaminated sediment may also expose benthic organisms through direct contact and ingestion. Subsequent uptake by aquatic organisms may facilitate bioaccumulation and the transfer of contaminants through the aquatic food web. Therefore, investigating both water and sediment matrices is necessary for a more comprehensive assessment of contaminant occurrence, mobility, and potential ecological effects.

The Jaboi geothermal area in Sabang is located within an outflow zone associated with active volcanic activity in Aceh Province, Indonesia. The geothermal manifestations in this area are characterized by fumaroles, hot mud pools, altered rocks, and dead vegetation. Four active craters are present, where fumaroles continuously release steam and geothermal gases. In addition to geothermal hot springs, several other water sources used by local communities are found in the surrounding area, including borehole water, dug wells, and treated water supplies. The Jaboi geothermal area is characterized by andesitic lava and pyroclastic rocks [9] with estimated reservoir temperatures of 196.9–416.5°C [10].

Previous studies in Indonesian geothermal systems have reported varying heavy metal concentrations, reflecting differences in reservoir characteristics and geological settings. In West Java, As concentrations range from 1 to 3,250 µg/L [11] and reach up to 6,500 µg/L, with Hg up to 6.5 µg/L [11]. In Talaga Bodas, Garut, As concentrations as high as 8,540 µg/L have been documented [12]. Closer to the study area, the Ie Se'um geothermal manifestation in Aceh Besar reported As concentrations of 0.80–166.73 µg/L in water and 2.56–6.86 mg/kg in sediment [13]. Despite these findings, no studies have been conducted on the occurrence and distribution of arsenic and mercury in the Jaboi geothermal area, which features active craters in close proximity to residential zones where local communities rely on various water sources for daily activities. The absence of baseline data raises significant concerns about potential exposure risks to the local population and surrounding ecosystem.

As and Hg were selected as the priority analytes for this study for several reasons. First, both elements are commonly enriched in geothermal systems worldwide due to their mobility in high-temperature fluids and their association with sulfide minerals [4, 5]. Second, they are among the most toxic heavy metals, with well-documented adverse health effects including carcinogenicity (As) and neurotoxicity (Hg) [6, 7]. Third, both elements are regulated by Indonesian water quality standards (Ministry of Health Regulation No. 32 of 2017), providing clear benchmarks for assessing potential health risks. Finally, their contrasting geochemical behaviors- As tends to adsorb onto sediments while Hg is more volatile- make them useful indicators for understanding metal mobility and fate in geothermal environments.

To address this knowledge gap, this study investigated As and Hg concentrations in water and sediment samples from the Jaboi geothermal area using Inductively Coupled Plasma–Optical Emission Spectrometry (ICP–OES), with method validation to ensure analytical reliability. The specific objectives were: (1) to quantify As and Hg concentrations in water samples, including hot springs, pools, stream channels, boreholes, dug wells, and treated water, and sediment samples collected from craters and stream beds; (2) to validate the ICP–OES method by evaluating linearity, limits of detection and quantification, precision, and accuracy; (3) to evaluate compliance with applicable environmental quality standards, including the Indonesian water-quality standards and the NOAA Sediment Quality Guidelines, Effects Range-Low (ERL) and Effects Range-Median (ERM), for sediment; (4) to compare As and Hg concentrations among sampling locations using one-way analysis of variance (ANOVA); and (5) to evaluate spatial distribution patterns and identify likely sources of these elements. Because the ANOVA was based on triplicate analytical measurements from a single grab sample at each location rather than independent field replicates, the statistical results were interpreted as exploratory comparisons of measured concentrations and analytical variability, rather than definitive evidence of spatial differences. It was hypothesized that geothermal activity is a likely source of As and Hg enrichment, with measured concentrations generally decreasing with increasing distance from the crater sources due to dilution, sedimentation, and adsorption processes. The findings are expected to

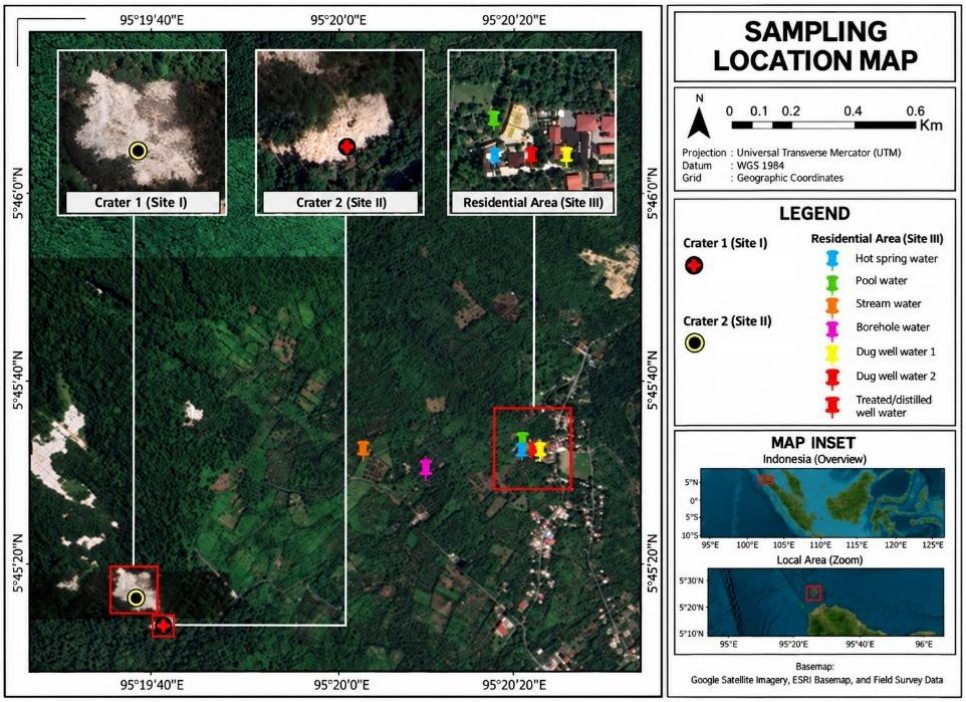


Figure 1. Water and sediment sampling locations in the Jaboi Geothermal Area, Sabang, based on Google Earth satellite imagery.

provide baseline information for environmental management and subsequent public-health assessment in the Jaboi area.

2. Materials and Methods

2.1. Time and Place of Research

This research was conducted at the Research Laboratory and Analytical Chemistry Laboratory, Department of Chemistry, Faculty of Mathematics and Natural Sciences, Universitas Syiah Kuala, Banda Aceh, from February to June 2025/2026.

2.2. Tools and Materials

The instruments used in this study included an Inductively Coupled Plasma–Optical Emission Spectrometry (ICP–OES), a microwave digestion system, a temperature and pH meter, a TDS meter, a conductivity meter, 500 mL polyethylene bottles, glass funnels, dropping pipettes, micropipettes, 100 mL volumetric flasks, measuring cylinders, beakers, a cool box, a stainless-steel spoon, and a plastic dipper. The materials used in this study were argon gas, filter paper, plastic clips, HCl, H_2O_2, 65% HNO_3, $Hg(NO_3)_2$, and H_3AsO_4.

2.3. Sample

The samples in this study were hot spring water (J1), pool water (J2), stream water (J3), borehole water (J4), dug well water 1 (J5), dug well water 2 (J6), treated/distilled well water (J7), and sediments from Crater 1 (SK1), Crater 2 (SK2), and stream sediment (SA) in the Jaboi Geothermal area, Sabang.

2.4. Sampling Location

Samples were obtained from the Jaboi Geothermal area, Sabang, which includes two main locations: Crater 1 and Crater 2 for hot spring water and sediment sampling (Figure 1). In this geothermal area, there is a hot spring bathing pool and a stream channel flowing from upstream to downstream, located not far from the hot spring source and residential areas. The local community also utilizes water for daily needs, including dug well water, borehole water, and treated well water.

Samples were collected from three sites: Crater 1 (Site I), Crater 2 (Site II), and the residential area (Site III). Hot spring water was obtained from Crater 2. Pool water, stream water, dug well water, borehole water, and treated well water were collected from the residential area. Sediment samples were obtained from Crater 1, Crater 2, and the stream channel. The sampling locations were selected purposively to represent different environmental zones along a potential pathway from the geothermal manifestations toward the residential area. Crater 1 (Site I) and Crater 2 (Site II) were selected to represent the geothermal-source zones, while the residential area (Site III) was selected to represent locations where surrounding water sources are used by the local community. J3 and SA were collected from the stream channel to represent the potential surface-water

Table 1. Sampling sites and sample types in the Jaboi geothermal area, Sabang.

Location (Site)	Sample Code	Sample Type	Coordinates
Crater 1 (Site I)	SK 1	Sediment	5°47′53″ N; 95°19′41″ E
Crater 2 (Site II)	J1	Hot spring water	5°47′56″ N; 95°19′38″ E
	SK 2	Sediment	
Residential Area (Site III)	J2	Hot spring pool water	5°48′12″ N; 95°20′21″ E
	J3	Stream water	5°48′13″ N; 95°20′21″ E
	SA	Stream Sediment	
	J4	Borehole water	5°48′12″ N; 95°20′03″ E
	J5	Dug well water 1	5°48′10″ N; 95°20′10″ E
	J6	Dug well water 2	5°48′12″ N; 95°20′23″ E
	J7	Treated/distilled well water	5°48′12″ N; 95°20′22″ E

and sediment transport pathway between the geothermal area and the downstream residential zone. J4–J7 represented groundwater and treated-water sources used in the residential area. This design was intended to provide an initial comparison among geothermal-source, transport-pathway, and residential-use zones rather than a spatially comprehensive survey. Because only seven water and three sediment locations were sampled, the design cannot fully characterize spatial variability across the Jaboi geothermal area. The sampling locations and sample types are presented in Table 1.

2.5. Research Procedures

2.5.1. Water Sampling

Water samples were collected using a plastic dipper and transferred into 500 mL polyethylene bottles that had been previously cleaned and rinsed with nitric acid. Prior to sample collection, each bottle was rinsed three times with the sample water. In situ measurements were performed immediately at each sampling point using portable instruments, including temperature, pH, TDS, salinity, and geographic coordinates. For laboratory analysis, water samples were preserved by adding nitric acid until pH < 2 and placed in a cool box containing ice packs during transportation to the laboratory (SNI, 2019). The preserved samples were then allowed to reach room temperature prior to ICP-OES analysis; no additional digestion was performed as acidification was sufficient for dissolved metal analysis.

2.5.2. Sediment Sampling

Sediment samples were collected using a stainless-steel spoon from Crater 1, Crater 2, and the stream channel. During sampling, the sampler faced upstream to minimize contamination from disturbed sediments. The collected samples were placed into sealable plastic bags and labeled according to their respective sample codes.

Sediment samples were dried at room temperature until dry and reported on a dry-weight basis (µg/kg dry weight). Samples were cleaned of foreign materials such as plastic fragments, leaves, and other debris. The samples were homogenized by grinding using a stainless-steel spoon until homogeneous. Approximately 1 g of each homogenized sample was weighed and transferred into a microwave digestion vessel. Subsequently, 5 mL of HNO_3 (p.a.), 1 mL of HCl (p.a.), and 1 mL of H_2O_2 (p.a.) were added. The samples were digested using a microwave digestion system until complete dissolution was achieved. After digestion, the solutions were allowed to cool, filtered, and diluted to a final volume of 100 mL with deionized water in a volumetric flask prior to analysis.

2.5.3. Interview

Face-to-face interviews were conducted with four residents of the Jaboi geothermal area, Sabang, who use local water sources for their daily activities. The informants utilized various water sources, including dug well water, borehole water, stream water, treated well water, and hot spring pool water. The interviews were conducted to obtain information on water-use practices and community perceptions regarding the quality and utilization of local water resources.

2.5.4. Arsenic and Mercury Analysis by ICP-OES

Prepared samples were analyzed using an Inductively Coupled Plasma–Optical Emission Spectrometry (ICP-OES) instrument (PerkinElmer Optima 8000, USA) equipped with WinLab32 software for data acquisition and processing. The operating conditions were as follows: RF power: 1.5 kW; plasma gas flow (argon): 8 L/min; auxiliary gas flow: 0.2 L/min; nebulizer gas flow: 0.7 L/min; sample uptake rate: 1.0 mL/min; viewing mode: axial. Arsenic was measured at 189.042 nm and mercury at 194.227 nm. Measurements were performed in triplicate for each sample. Direct solution nebulization was employed; no hydride generation or cold vapor accessory was used for either element [15].

Table 2. Equations used for method validation.

Name	Formula	References
Regression standard deviation	$S_r = \sqrt{\frac{S_{yy} - m^2 S_{xx}}{N-2}}$	[13, 14]
Slope standard deviation	$S_m = \sqrt{\frac{S_r^2}{\sum(\bar{X} - X_i)^2}}$ $= \sqrt{\frac{S_r^2}{\sum x_i^2 - (\sum X_i)^2 / N}}\bar{X}$	
Intercept standard deviation	$S_b = S_r = \sqrt{\frac{S_r^2 \sum x_i^2}{N\sum x_i^2 - (X_i)^2}}$ $= \sqrt{\frac{1}{N - (\sum x_i^2 / \sum x_i^2}}$	
Concentration standard deviation	$S_C = \frac{S_r}{m}\sqrt{\frac{1}{M} + \frac{1}{N} + \frac{(YC - Y_{ave})^2}{m^2 S_{xx}}}$	
Limit of Detection	LoD = 3,3 $(\frac{\sigma}{slope})$	
Limit of Quantification	LoQ = 10 $(\frac{\sigma}{slope})$	

2.5.5. Preparation of Arsenic (As) Standard Solutions

A 1000 mg/L H_3AsO_4 standard solution was used as the stock solution. An intermediate standard solution of 100 mg/L was prepared by pipetting 10 mL of the stock solution into a 100 mL volumetric flask and diluting to volume with 5% HNO_3. Next, an intermediate standard solution of 1 mg/L was prepared by pipetting 1 mL of the 100 mg/L solution into a 100 mL volumetric flask and diluting to volume. From the 1 mg/L standard solution, a 100 µg/L standard solution was prepared by pipetting 10 mL into a 100 mL volumetric flask and diluting to volume. This 100 µg/L solution was then used to prepare a standard series with concentrations of 5, 10, 50, and 100 µg/L by pipetting appropriate volumes into 100 mL volumetric flasks and diluting with deionized water containing 1.5 mL/L HNO_3 to the mark. Standard solutions were ready for analysis using ICP-OES.

2.5.6. Preparation of Mercury (Hg) Standard Solutions

A 1000 mg/L $Hg(NO_3)_2$ standard solution was used as the stock solution. An intermediate standard solution of 100 mg/L was prepared by pipetting 10 mL of the stock solution into a 100 mL volumetric flask and diluting to volume with 5% HNO_3. Next, an intermediate standard solution of 1 mg/L was prepared by pipetting 1 mL of the 100 mg/L solution into a 100 mL volumetric flask and diluting to volume. From the 1 mg/L standard solution, a 100 µg/L standard solution was prepared by pipetting 10 mL into a 100 mL volumetric flask and diluting to volume. This 100 µg/L solution was then used to prepare a standard series with concentrations of 2.5, 5, 10, and 50 µg/L by pipetting appropriate volumes into 100 mL volumetric flasks and diluting with deionized water containing 1.5 mL/L HNO_3 to the mark. Standard solutions were ready for analysis using ICP-OES.

2.5.7. Calibration Curve Preparation

Calibration curves for As and Hg were obtained by measuring the signal intensity (cps) of each metal at each standard concentration. As standard concentrations were 5, 10, 50, and 100 µg/L; Hg standard concentrations were 2.5, 5, 10, and 50 µg/L.

2.5.8. Linearity Assessment

Linear regression analysis was performed using the least-squares method (LINEST) in Microsoft Excel. Standard deviation (SD) values and calibration data were used to obtain statistical parameters, including the coefficient of determination (R^2), slope (m), intercept (b), and their associated standard deviations. These parameters were subsequently used for method validation and the evaluation of measurement uncertainty [16]. The equations employed in the calculations are presented in Table 2.

Linearity was assessed using the correlation coefficient (r) and coefficient of determination (R^2) obtained from the calibration curves of As and Hg at six concentration levels (0, 5, 10, 50, and 100 µg/L for As; 0, 2.5, 5, 10, and 50 µg/L for Hg). A calibration curve was considered acceptable when $0.95 < r < 0.99$ and excellent when $r > 0.99$ [13].

2.5.9. Limit of Detection (LoD) and Limit of Quantification (LoQ)

The LoD and LoQ were calculated from the regression parameters of the calibration curves using the equations

in Table 2 [17], where S_b is the standard deviation of the intercept of the regression line, and slope is the slope of the calibration curve.

2.5.10. Precision

Precision was evaluated by analyzing standard solutions in triplicate and expressed as the relative standard deviation (%RSD) [18]. A method was considered precise when %RSD values met the AOAC 2002 guidelines or the 2/3 Horwitz coefficient of variation (CV Horwitz) criterion [19].

2.5.11. Accuracy (Spike-Recovery)

Accuracy was determined through spike recovery experiments. Approximately 1 g of sediment sample was spiked with As and Hg standard solutions at a concentration of 10 µg/L prior to digestion, then processed through the same digestion and analysis procedure as unspiked samples. Measurements were performed in triplicate using ICP-OES. Percent recovery was calculated using Equation (1):

$$Recovery\ (\%) = \frac{\bar{X}}{\mu} \times 100 \quad (1)$$

Where $\bar{X}$ is the average measured concentration from triplicate measurements and μ is the true concentration (spike concentration added, 10 µg/L). Recovery values within the range of 70–125% were considered acceptable.

Sediment concentrations were compared with the NOAA Effects Range-Low (ERL) and Effects Range-Median (ERM) values as ecological screening benchmarks. The ERL and ERM were used to screen the potential for effects on sediment-associated organisms and were not interpreted as human-health standards. Indonesian water-quality benchmarks were considered separately according to the intended or reported use of the water samples.

2.5.12. Statistical Analysis

One-way ANOVA was used to compare the analytical measurements obtained from samples collected at different locations. For water samples, the analysis included seven groups (J1–J7), with three analytical measurements per sample. For sediment samples, the analysis included three groups (SK1, SK2, and SA), with three analytical measurements per sample. The statistical results were reported using the available F statistics, degrees of freedom, and p-value thresholds.

The triplicate measurements were repeated analytical measurements of a single grab sample from each location rather than independently collected field replicates. Therefore, the independence assumption required for population-level spatial inference was not satisfied. Because only three analytical measurements were available for each sample, the normality and homogeneity assumptions could not be evaluated robustly. Consequently, the ANOVA results were treated as exploratory comparisons among the analysed samples relative to analytical variability and were not interpreted as definitive evidence of spatial differences. Statistical significance was evaluated at p = 0.05.

3. Results and Discussion

3.1. In Situ Analysis

In situ measurements were conducted at each sampling site to determine physicochemical parameters, including pH, total dissolved solids (TDS), electrical conductivity (EC), temperature, and salinity.

The in situ analysis results are presented in Table 3. Samples J1, J2, and J3 exhibited pH values below the applicable water quality standards, whereas samples J4–J7 complied with the recommended limits. Elevated TDS concentrations were observed in J1 and J2, while J3 exceeded the drinking water standard but remained within the acceptable range for clean water. Samples J4–J7 met the TDS requirements for both clean water and drinking water. The EC values of several samples fell outside the recommended ranges, indicating variations in dissolved ionic content among the sampling sites. Regarding temperature, sample J7 complied with the applicable standard, whereas the remaining samples showed elevated temperatures due to geothermal influence. Salinity was highest in J1 and lowest in J7, suggesting a gradual reduction in dissolved salts from geothermal sources toward residential water supplies. Elevated salinity levels may adversely affect water quality and pose potential health risks when present above acceptable limits [20].

Several patterns emerge when the physicochemical parameters are considered in relation to the measured As and Hg concentrations. Sample J1 exhibited the lowest pH (2.63), highest temperature (75.50°C), and highest TDS concentration (2,942.0 mg/L), together with the highest measured As and Hg concentrations. The acidic conditions may promote the dissolution of metal-bearing minerals and facilitate the release of As and Hg into solution [21]. Conversely, samples with near-neutral pH and lower temperatures generally showed lower measured metal concentrations. These observations are consistent with geothermal influence; however, they

Table 3. Results of in situ measurements of water samples.

No.	Sample	pH ± SD	TDS ± SD (mg/L)	EC ± SD (µS/cm)	Temperature ± SD (°C)	Salinity ± SD (‰)
1	J1	2.63 ± 0.03	2942.0 ± 560.1	5922.0 ± 722.5	75.50 ± 0.07	12.1 ± 2.31
2	J2	6.22 ± 0.02	1004.2 ± 8.4	1941.2 ± 5.0	51.32 ± 0.02	3.7 ± 0.15
3	J3	6.43 ± 0.02	353.6 ± 2.2	688.6 ± 1.1	38.28 ± 0.09	1.5 ± 0.09
4	J4	6.83 ± 0.02	203.0 ± 1.6	405.0 ± 1.9	32.29 ± 0.05	0.9 ± 0.08
5	J5	7.09 ± 0.03	99.5 ± 0.2	199.4 ± 0.3	30.23 ± 0.03	0.5 ± 0.11
6	J6	7.21 ± 0.02	171.4 ± 6.7	207.9 ± 0.5	31.17 ± 0.03	0.5 ± 0.08
7	J7	7.18 ± 0.02	25.6 ± 1.3	3.2 ± 0.2	29.88 ± 0.05	0.2 ± 0.11
Clean water standard*	6.5–9.0	1000	30–200	25–29	0.50	
Drinking water standard*	6.5–8.5	500	1500	10–25	0.05	

*Note: Temperature standards apply to drinking water and clean water sources intended for domestic use. Hot spring water (J1) and pool water (J2) are geothermal features not intended for consumption; their elevated temperatures are consistent with geothermal activity and do not indicate non-compliance with domestic water standards.

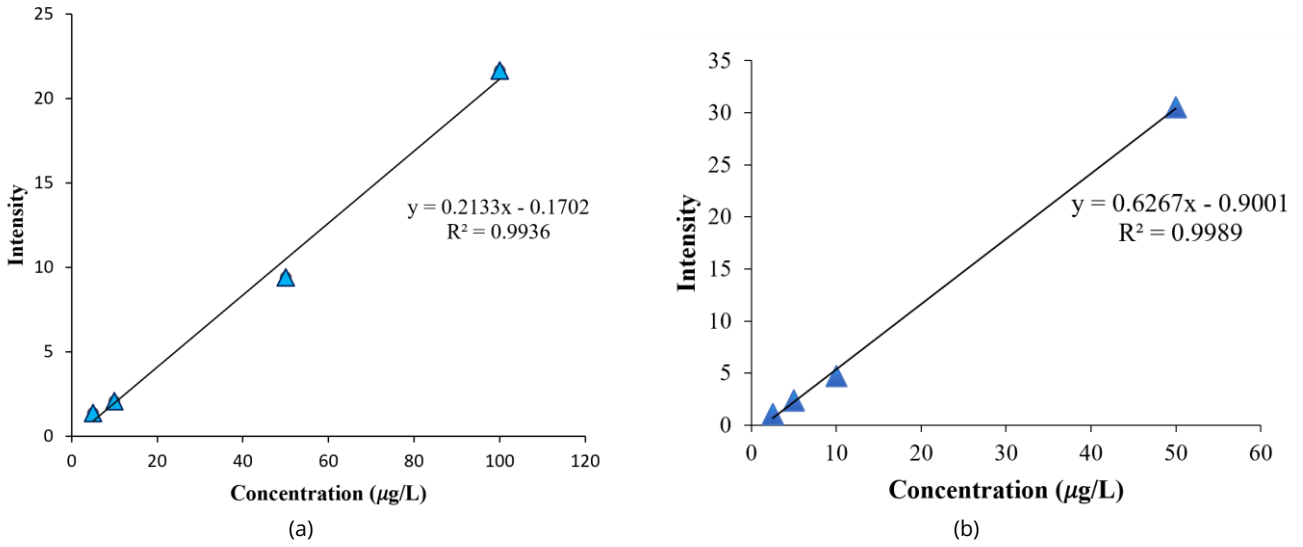


Figure 2. Calibration curves for (a) arsenic and (b) mercury standards.

should be interpreted as descriptive associations because no formal correlation analysis was performed.

3.2. Method Validation

3.2.1. Calibration Curve and LoD/LoQ

The calibration curves for As and Hg are presented in Figure 2. The linearity of the calibration curves was assessed using the coefficient of determination (R^2). Values between 0.95 and 0.99 indicate good linearity, whereas values greater than 0.99 indicate excellent linearity [13].

The calibration curves showed R^2 values of 0.9936 for As and 0.9989 for Hg, as determined by linear regression analysis using Microsoft Excel. The corresponding regression parameters and statistical characteristics, including slope, intercept, and standard deviations, are summarized in Table 4. These results indicate excellent linearity between the concentrations of the standard solutions and the corresponding instrument responses, confirming the suitability of the method for the determination of As and Hg.

Based on the calibration data, the LoD and LoQ were calculated statistically using the LINEST function in Microsoft Excel [22]. The calculated LoD and LoQ values are presented in Table 5.

Under the analytical conditions used in this study, the calculated LoD and LoQ were lower for Hg than for As. This observation is limited to the selected wavelengths, calibration ranges, direct-nebulization conditions, and instrument configuration. It should not be interpreted as demonstrating that ICP–OES is universally more sensitive for Hg than for As.

3.2.2. Precision and Accuracy

Precision was evaluated through repeated measurements of the analytes. A method is considered precise when repeated analyses produce results with minimal variation [23]. Table 6 summarizes the precision

Table 4. Linearity and uncertainty of the calibration curves.

Name	Result	
	As	Hg
Slope	0.213278195	0.626672251
Intercept	-0.17022556	-0.90009424
Standard Deviation of Slope (S_m)	0.012067723	0.014692599
Standard Deviation of Intercept (S_b)	0.677970867	0.376833661
Coefficient of Determination (R^2)	0.993637676	0.998901831
Standard Deviation of Regression (S_r)	0.920534742	0.567558102
Sum of Square Regression	264.6809066	586.0090556
Sum of Square Residual	1.694768421	0.644244398

Table 5. Limit of Detection (LoD) and Limit of Quantification (LoQ).

Parameter	As (µg/L)	Hg (µg/L)
LoD	10.49	1.98
LoQ	31.78	6.01

Table 6. Precision and %Recovery of As and Hg in sediment samples.

No	Sample	% Recovery		RSD (%)	
		As	Hg	As	Hg
1	Replicate 1	111.312	116.21	1.410	6.635
2	Replicate 2	119.104	120.45		
3	Replicate 3	96.598	99.24		

and recovery results obtained from sediment samples spiked with As and Hg standard solutions at a concentration of 10 µg/L. The individual recovery values are reported for each replicate, while the relative standard deviation (RSD) represents the precision calculated for each analyte from repeated measurements.

Validation was performed using the sediment matrix only; water-matrix recovery and precision were not independently evaluated. Therefore, the validation results should not be interpreted as demonstrating equivalent analytical performance in water samples.

The recovery values for both As and Hg were within the acceptable range of 70–125%. Mercury exhibited a higher recovery than arsenic, which may be associated with its volatile nature and the potential influence of volatilization on analytical measurements. The precision of As was considered satisfactory, as indicated by a %RSD value below 2%. Although the %RSD value of Hg exceeded 2%, it still met the 2/3 Horwitz coefficient of variation (CV Horwitz) criterion and was therefore considered acceptable. Similar findings were reported by Juliasih et al. [19], who observed %RSD values above 2% for Cd, Cr, Cu, Ni, Co, and Mn; however, these values remained below the corresponding 2/3 CV Horwitz limits, indicating good analytical precision. These results demonstrate that the analytical method used in this study provides acceptable precision and accuracy for the determination of As and Hg.

It should be noted that method validation (recovery and precision) was performed using spiked sediment samples only. Recovery and precision data for water samples were not independently validated due to the low As concentrations approaching the detection limit. Matrix effects may differ between sediment and water matrices, and the recovery values reported may not fully represent analytical performance in aqueous samples. Future studies should include water-matrix spike-recovery experiments at multiple concentration levels to confirm analytical accuracy for water samples. Despite this limitation, the linearity, LoD, and LoQ parameters established through calibration standards are applicable to both matrices as they reflect instrument performance rather than matrix-specific effects.

3.3. Analysis of As and Hg in Water Samples

The highest As instrument response was observed in J1 and corresponded to an estimated concentration of 11.268 ± 3.370 µg/L. Because this value was above the LoD of 10.49 µg/L but below the LoQ of 31.78 µg/L, As was detected in J1 but could not be reliably quantified. The analyzed samples represented various water sources, including geothermal and domestic water supplies.

The concentrations of As and Hg measured in the water samples are presented in Table 7. The highest As concentration was detected in sample J1 (hot spring water) at 11.268 ± 3.370 µg/L. This sample exceeded the drinking water quality standard of 10 µg/L but remained below the clean water standard of 50 µg/L. For all other

Table 7. Arsenic (As) and mercury (Hg) concentrations in water samples collected from the Jaboi Geothermal Area.

No	Code Sample	As (µg/L)	Status	Hg (µg/L)
1	J1	11.268 ± 3.370	Detected; not reliably quantified	6.861 ± 0.700
2	J2	< LoD (10.49)	Not quantified	1.649 ± 0.754
3	J3	< LoD (10.49)	Not quantified	3.404 ± 0.703
4	J4	< LoD (10.49)	Not quantified	1.915 ± 0.748
5	J5	< LoD (10.49)	Not quantified	1.755 ± 0.753
6	J6	< LoD (10.49)	Not quantified	2.021 ± 0.749
7	J7	< LoD (10.49)	Not quantified	1.596 ± 0.755
Clean water quality standard*		50 µg/L		1 µg/L
Drinking water quality standard*		10 µg/L		1 µg/L

*Based on the Indonesian Ministry of Health Regulation (Permenkes RI) No. 32 of 2017.
Note: J1 (hot spring water); J2 (hot spring pool water); J3 (stream water); J4 (borehole water); J5 (dug well water 1); J6 (dug well water 2); and J7 (treated well water).

water samples (J2–J7), As concentrations were below the method's limit of detection (10.49 µg/L); these values cannot be reliably quantified and are reported as < LoD. Consequently, interpretations of As spatial gradients should be limited to the qualitatively detectable trend from J1 to other locations rather than quantitative comparisons among J2–J7. The elevated As level in J1 is likely associated with geothermal activity, which promotes the dissolution and mobilization of arsenic-bearing minerals.

Mercury produced the highest instrument response in J1 (hot spring water), corresponding to an estimated concentration of 6.861 ± 0.700 µg/L, followed by J3 (stream water), with an estimated concentration of 3.404 ± 0.703 µg/L. The higher Hg response observed in J1 is consistent with possible geothermal influence, although the available data do not exclude other natural or anthropogenic sources. Interpretation of the Hg results must consider the method LoD of 1.98 µg/L and LoQ of 6.01 µg/L. Only J1 had an Hg concentration above the method LoQ and could therefore be quantified reliably. Hg was detected but not reliably quantified in J3 and J6 because their measured responses corresponded to concentrations between the LoD and LoQ, whereas J2, J4, J5, and J7 were below the method LoD. Because the applicable Hg standard of 1 µg/L is lower than the method LoD, this ICP–OES method was not sufficiently sensitive to confirm compliance or exceedance for samples other than J1. Consequently, exceedance of the Hg standard could not be confirmed reliably for all samples. The quantifiable Hg exceedance in J1 remains an environmental concern because prolonged Hg exposure may cause adverse health effects [24, 25]. Confirmation of the remaining samples requires a more sensitive Hg-specific analytical method, such as cold-vapor atomic absorption spectrometry, cold-vapor atomic fluorescence spectrometry, or ICP–MS.

The Indonesian Ministry of Health Regulation No. 32 of 2017 establishes two tiers of water quality standards: drinking water standards (As: 10 µg/L, Hg: 1 µg/L) and clean water standards for hygiene/sanitation purposes (As: 50 µg/L, Hg: 1 µg/L). In this study, drinking water standards were applied to samples used for consumption (boreholes J4, dug wells J5 and J6, treated water J7), while clean water standards were applied to samples used for bathing and washing (pool J2, stream J3). Sample J1 (hot spring) is a geothermal feature not intended for any domestic use; comparison with drinking water standards is presented only as a screening reference. Similarly, the elevated temperature of J1 (75.50°C) is consistent with geothermal activity and does not indicate non-compliance with domestic water temperature standards (10–25°C), which are intended for drinking water sources only.

3.4. Analysis of As and Hg in Sediment Samples

As and Hg levels in sediment samples were analyzed using ICP-OES to determine the accumulation of heavy metals in the Jaboi Geothermal manifestation area, Sabang. Sediment samples were collected from Crater 1 (SK1), Crater 2 (SK2), and the channel (SA). The analysis results showed variations in As and Hg concentrations between sampling locations. NOAA (National Oceanic and Atmospheric Administration) scientists developed Sediment Quality Guidelines/SQG in the form of Effects Range-Low (ERL) and Effects Range-Median (ERM), which are used to help interpret the significance of the levels of chemical contaminants observed in sediment [26].

The concentrations of As and Hg in the sediment samples are presented in Table 8. The highest As concentration was detected in sample SK2 at 9.080 ± 3.842 µg/kg

Table 8. Arsenic (As) and mercury (Hg) concentrations in sediment samples collected from the Jaboi Geothermal Area.

No	Code Sample	As (µg/kg dry wt.)	Hg (µg/kg dry wt.)
1	SK1	2.360 ± 3.711	6.382 ± 0.703
2	SK2	**9.080** ± 3.842	6.648 ± 0.701
3	SA	1.891 ± 3.750	5.319 ± 0.711
NOAA Guideline		**As**	**Hg**
ERL		8.200 µg/kg	150 µg/kg
ERM		70.000 µg/kg	710 µg/kg

(equivalent to 9.08 mg/kg), which marginally exceeds the NOAA Effects Range-Low (ERL) value of 8,200 µg/kg (8.2 mg/kg) but remains well below the Effects Range-Median (ERM) value of 70,000 µg/kg (70 mg/kg). The ERL represents the lower 10th percentile of sediment concentrations associated with biological effects; concentrations below the ERL are within the "no effects range," while concentrations between the ERL and ERM fall within the "possible effects range," indicating potential for adverse ecological effects [26]. This finding suggests a potential for initial biological effects, although it does not indicate severe arsenic contamination. Mercury concentrations in sediments ranged from 5.319 to 6.648 µg/kg, substantially below the NOAA ERL of 150 µg/kg, indicating no significant mercury contamination in the sediments. Measurement uncertainty was higher for As (±3.711–3.842 µg/kg) than for Hg (±0.701–0.711 µg/kg), suggesting greater analytical stability for Hg measurements. This difference may be related to variations in method sensitivity for each element, particularly at relatively low concentrations.

The comparatively elevated responses at J1, together with its low pH, high temperature, and high TDS, are consistent with possible geothermal influence. However, the observed distribution does not independently confirm a spatial gradient or identify the source of As and Hg. Because the study did not include independent field replicates, background sites, or source-specific geochemical tracers, geothermal activity should be interpreted as a possible contributor rather than a confirmed primary source. The observed decline in metal concentrations at more distant locations may be associated with dilution processes, sedimentation, and the adsorption of metals onto sediments. The spatial distribution is characterized by a shift in color gradation from red-orange, indicating higher concentrations around the geothermal source, to green-blue, indicating lower concentrations in residential areas. Although this pattern suggests a potential influence of geothermal activity or geothermal manifestations in the crater area, further investigation is required to establish the primary source of heavy metal contamination.

Under the instrumental conditions used in this study, the calculated LoD and LoQ for Hg were 1.98 and 6.01 µg/L, respectively, compared with 10.49 and 31.78 µg/L for As. These results indicate that the method produced lower calculated detection and quantification limits for Hg than for As under the selected wavelengths, calibration ranges, and direct-nebulization conditions. However, this comparison should not be generalized as evidence that ICP–OES is universally more sensitive for Hg because analytical sensitivity depends on instrument configuration, wavelength selection, background correction, matrix effects, and calibration design.

Interviews with four residents were used only to obtain informal contextual information about local water-use practices and community perceptions. None of the interviewed residents reported health complaints that they associated with the use of local water sources. However, this observation should not be interpreted as evidence of the absence of adverse health effects or as an assessment of community health status. The small number of participants, the absence of clinical evaluation, and the lack of biomonitoring data prevent conclusions about health effects related to As or Hg exposure. Potential risks associated with chronic exposure therefore require evaluation through a properly designed epidemiological or health-risk assessment.

3.5. Statistical Analysis

Exploratory one-way ANOVA was performed separately for As and Hg in water and sediment samples. For water, the analysis included seven sample groups (J1–J7), with three analytical measurements for each sample, resulting in 21 observations. For sediment, the analysis included three sample groups (SK1, SK2, and SA), with three analytical measurements for each sample, resulting in nine observations. The F statistics, degrees of freedom, and available p-value thresholds are presented in Tables 9 and 10.

For water samples, the reported ANOVA results were $F(6,14) = 943.43$, $p < 0.001$ for As and $F(6,14) = 1010.32$, $p < 0.001$ for Hg. The large F statistics indicate that the differences among the measurements obtained from the individual water samples were substantially greater than the variation among repeated analytical measurements

Table 9. Exploratory ANOVA results for water samples.

Source	df	SS	MS	F calculated	p-value
Arsenic (As)					
Between locations	6	236.91	39.48	943.43	< 0.001
Within locations	14	0.59	0.04		
Total	20	237.50			
Mercury (Hg)					
Between locations	6	66.28	11.05	1010.32	< 0.001
Within locations	14	0.15	0.01		
Total	20	66.43			

Table 10. Exploratory ANOVA results for sediment samples.

Source	Df	SS	MS	$F_{calculated}$	p-value
Arsenic (As)					
Between locations	2	2.97	1.49	47.68	< 0.001
Within locations	6	0.19	0.03		
Total	8	3.16			
Mercury (Hg)					
Between locations	2	2.84	1.42	45.23	< 0.001
Within locations	6	0.19	0.03		
Total	8	3.03			

of the same sample. However, the As results require additional caution because J2–J7 were below the method LoD and could not be reliably quantified. Therefore, the As ANOVA should not be interpreted as demonstrating quantitative differences or a concentration gradient among J2–J7.

For sediment samples, the reported ANOVA results were $F(2,6) = 47.68$, $p < 0.001$ for As and $F(2,6) = 45.23$, $p < 0.001$ for Hg. These results indicate that the differences among the measurements obtained from SK1, SK2, and SA were greater than the variation among repeated analytical measurements of each sediment sample. Nevertheless, the analysis was based on only one grab sample from each location. Accordingly, the results describe differences among the specific samples analysed and cannot be generalized as population-level differences among the sediment locations.

Although the reported p-value thresholds were below the predetermined significance level of $p = 0.05$, the statistical results must be interpreted in relation to the replication structure. The three observations within each group were analytical replicates, representing repeated instrumental measurements of a single grab sample, rather than independently collected field replicates. Analytical replicates are useful for evaluating measurement repeatability, but they do not capture natural environmental variability within each sampling location.

Consequently, the ANOVA results should be treated as exploratory comparisons among the analysed grab samples relative to analytical variability. They do not independently confirm spatial differences, a source-to-residential concentration gradient, or geothermal activity as the source of the measured elements. Confirmation of spatial patterns would require multiple independent field samples from each location, additional sampling points, and repeated sampling across different periods or seasons.

It should be noted that each sample group consisted of three repeated analytical measurements from a single grab sample rather than independently collected field replicates. Therefore, the ANOVA results represent exploratory comparisons among the analysed samples relative to analytical variability and should not be interpreted as population-level spatial differences. The reported p-values are threshold values rather than exact calculated p-values. In addition, the As results for J2–J7 were below the method LoD and were not interpreted as reliable quantitative concentrations.

3.6. Discussion

3.6.1. Spatial Distribution and Source Attribution

The main discoveries of this study reveal that the highest concentrations of As (11.268 ± 3.370 µg/L) and Hg (6.861 ± 0.700 µg/L) were recorded at the hot spring site (J1), significantly higher than at other sampling locations (J2–J7), suggesting that geothermal activity is the likely primary source of these heavy metals. All water samples exceeded the mercury quality standard of 1 µg/L set by the Indonesian Ministry of Health Regulation No. 32 of 2017, raising concerns about potential health risks to local communities. In sediment samples, the highest As concentration at SK2 (9,080 ± 3,842 µg/kg) marginally exceeded the NOAA ERL value of 8,200 µg/kg, while Hg

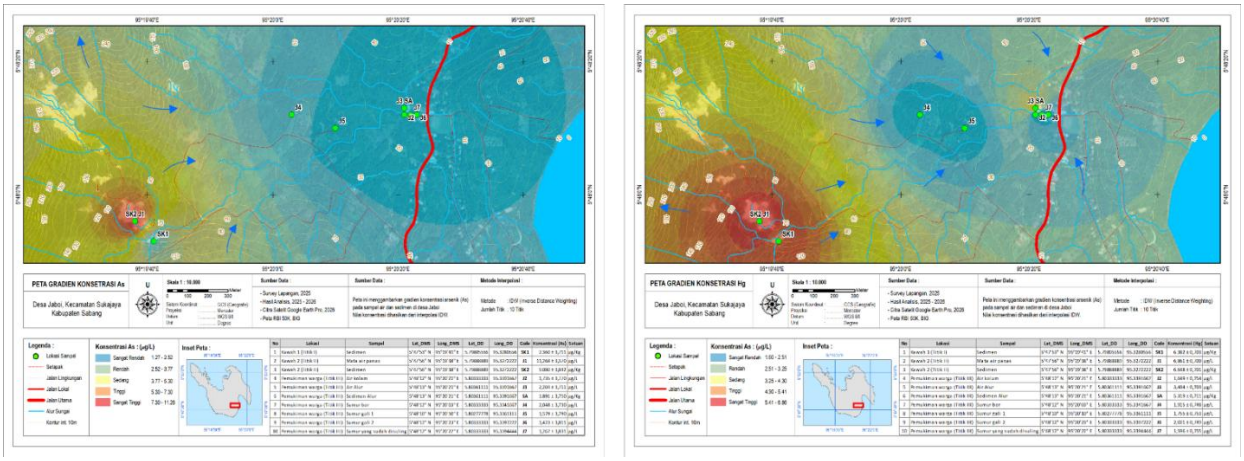


Figure 3. Sampling-point distribution of arsenic (As) and mercury (Hg) concentrations from the geothermal crater area toward the residential area in Jaboi, Sabang.

concentrations (5.319–6.648 µg/kg) remained well below the NOAA threshold of 150 µg/kg.

The spatial distribution pattern (Figure 3) clearly showed a decreasing trend in metal concentrations from the crater areas toward residential zones. The concentrations of As decreased from 11.268 µg/L at J1 (hot spring) to below the detection limit at J7 (treated well water). Similarly, Hg concentrations decreased from 6.861 µg/L at J1 to 1.596 µg/L at J7, representing a reduction of approximately 76.7%. This progressive dilution provides strong evidence that geothermal sources are the primary contributors, with dilution, sedimentation, and adsorption processes gradually reducing concentrations as water flows downstream.

The measured conditions at J1, including low pH, high temperature, high TDS, and comparatively elevated As and Hg responses, are consistent with geothermal influence and with the reported geochemical behaviour of these elements in geothermal environments [5, 27]. However, these observations do not by themselves establish geothermal activity as the source of the measured elements at all sampling locations. The study did not include major-ion chemistry, sulfate, chloride, isotopic tracers, mineralogical analysis, background reference sites, or other source-specific indicators. Therefore, alternative natural and anthropogenic sources cannot be excluded. Geothermal activity should consequently be interpreted as a possible or likely contributor to the observed metal enrichment rather than as a confirmed primary source. Confirmation would require independent field replication and additional geochemical source tracers.

3.6.2. Comparison with Previous Studies

A comparison of these findings with previous studies in Indonesia reveals both similarities and differences. The As concentration in Jaboi hot spring (11.268 µg/L) was considerably lower than those reported in Talaga Bodas, Garut (up to 8,540 µg/L; [12] and the Ciwidey watershed (1–3,250 µg/L; [11]. However, it was still within the range of values reported in the Ie Se'um geothermal area, Aceh (0.80–166.73 µg/L; [13]. For mercury, the concentration in Jaboi (6.861 µg/L) was slightly higher than that reported in West Java geothermal waters (6.5 µg/L; [11], but remained comparable to values found in other active geothermal systems globally [21].

The unexpectedly lower As concentrations in Jaboi compared to Talaga Bodas and Ciwidey may be attributed to differences in geothermal reservoir characteristics. The Jaboi system is characterized as an outflow zone with relatively lower temperatures compared to the magmatic-hydrothermal systems found in West Java and Garut. At lower temperatures, the dissolution rates of arsenic-bearing minerals such as arsenopyrite and pyrite are reduced, resulting in lower arsenic concentrations in geothermal fluids [28]. Additionally, differences in local lithology and the mineral composition of host rocks play a crucial role; areas with higher abundance of arsenic-bearing minerals tend to release more arsenic into geothermal fluids. The depth and circulation patterns of geothermal fluids also affect the contact time between fluids and arsenic-bearing rocks, influencing the final concentrations observed at surface manifestations.

The higher Hg concentration in Jaboi compared to West Java, despite lower As levels, may be explained by the different geochemical behaviors of these two elements. Mercury is highly volatile and can be released through fumarolic activity at the four active craters in Jaboi, contributing to elevated concentrations in surface waters [4]. The continuous emission of Hg from geothermal vents likely maintains elevated aqueous concentrations

even when reservoir temperatures are relatively lower. In contrast, arsenic mobilization is more dependent on temperature-dependent dissolution processes, explaining why As concentrations are lower in cooler outflow zones.

3.6.3. Implications for Environmental Management and Public Health

The finding that all water samples exceeded the Hg quality standard of 1 µg/L indicates that current water sources used by local communities may pose potential long-term health risks, including neurological impairment and kidney dysfunction [7], despite no health problems being reported to date. The detection of As in sediment at levels exceeding the NOAA ERL also suggests potential ecological risks, warranting further investigation. The spatial distribution patterns observed in this study, combined with statistical confirmation through ANOVA, establish a clear relationship between geothermal activity and heavy metal contamination in the region. This has important implications for understanding heavy metal dispersion in geothermal areas and for developing appropriate management and mitigation strategies.

Several limitations of this study should be acknowledged. First, method validation was performed on sediment matrices only; water-matrix validation is needed to confirm analytical accuracy for aqueous samples. Second, most As concentrations in water were below the detection limit, precluding reliable quantification and interpretation. Third, ANOVA results are based on analytical replicates (triplicate instrument readings) rather than independent field replicates, limiting their ability to confirm spatial trends. Fourth, the small number of sampling sites (7 water, 3 sediment) may not fully represent spatial and temporal variability. Fifth, interviews with only four residents are insufficient to establish public health status and should be interpreted as informal contextual information only.

4. Conclusions

The highest As and Hg responses were observed in the hot-spring sample J1. The As response in J1 was above the method LoD but below the LoQ and was therefore not reliably quantified, while As in J2–J7 was below the LoD. For Hg, only J1 was above the method LoQ and showed a quantifiable exceedance of the 1 µg/L screening benchmark. Compliance or exceedance could not be confirmed for the remaining water samples because the benchmark was below the method LoD. The measured conditions at J1 are consistent with possible geothermal influence, but source attribution cannot be confirmed without independent field replication, background locations, and additional geochemical tracers.

In sediments, the highest As concentration at SK2 (9,080 µg/kg dry weight) marginally exceeded the NOAA Effects Range-Low (ERL) value of 8,200 µg/kg, suggesting potential for initial biological effects, while mercury concentrations in all sediment samples (5.319–6.648 µg/kg) remained well below the NOAA ERL threshold of 150 µg/kg, indicating no significant Hg contamination in sediments. The observed results were consistent with generally lower metal concentrations away from the geothermal source. However, a quantitative percentage decrease could not be calculated reliably for As because most water samples were below the method detection limit. This pattern should be interpreted cautiously because of the limited number of sampling locations and the absence of independent field replicates.

The ICP-OES method demonstrated acceptable validation parameters for sediment matrix analysis, with excellent linearity ($R^2 > 0.99$), recovery values within 70–125%, and precision within acceptable limits; however, validation for water matrices was not independently performed, and this limitation should be considered when interpreting aqueous As results, particularly those near the detection limit. Although interviews with local residents revealed no reported health issues linked to As or Hg exposure, the finding that all water samples exceeded the Hg quality standard indicates potential long-term health risks that warrant regular monitoring and expanded health risk assessments.

Several limitations of this study should be acknowledged. Method validation was performed on sediment matrices only; water-matrix validation is needed to confirm analytical accuracy for aqueous samples. Most As concentrations in water (J2–J7) were below the detection limit (10.49 µg/L), precluding reliable quantification and interpretation. ANOVA results for water samples are based on analytical replicates (triplicate instrument readings) rather than independent field replicates, limiting their ability to confirm spatial trends. The small number of sampling sites (7 water, 3 sediment) may not fully represent spatial and temporal variability in the study area. Interviews with only four residents are insufficient to establish public health status and should be interpreted as informal contextual information only.

Despite these limitations, this study provides the first comprehensive baseline data on As and Hg contamination in both water and sediment from the Jaboi geothermal area, with mercury in water identified as the primary environmental concern. The spatial distribution pattern suggests geothermal activity as the likely primary source of contamination, with concentrations decreasing with distance from the crater sources. The findings establish a foundation for future monitoring programs

and health risk assessments in the area. Based on these findings, future research should include seasonal variation studies to understand the influence of rainfall, temperature, and water flow on metal concentrations; comprehensive health risk assessments including analysis of As and Hg in human biological samples (hair, urine) and aquatic biota (fish) to evaluate actual human exposure; the use of more sensitive analytical techniques such as ICP-MS or HG-AAS for As determination at low concentrations; and the establishment of long-term monitoring programs to track changes in metal concentrations over time, as well as expansion of sampling area and number of points around the geothermal manifestation to obtain more detailed information on spatial distribution patterns.

Author Contributions: Conceptualization, F.B. and R.I.; methodology, F.B.; software, F.B.; validation, F.B., R.I. and L.L.; formal analysis, F.B.; investigation, F.B.; resources, R.I.; data curation, F.B.; writing—original draft preparation, F.B.; writing—review and editing, F.B., R.I. and L.L.; visualization, F.B.; supervision, R.I. and L.L.; project administration, R.I.; funding acquisition, R.I. All authors have read and agreed to the published version of the manuscript.

Funding: This study does not receive external funding.

Ethical Clearance: Not applicable.

Informed Consent Statement: Not applicable.

Data Availability Statement: The data supporting the findings of this study are available from the corresponding author upon reasonable request

Conflicts of Interest: All the authors declare no conflicts of interest.

References

1. Pinning, F., Haryanto, A. D., and Hutabarat, J. (2023). Hydrogeochemistry and Isotope Characteristics of the Hot Springs in the Wapsalit Area, Buru Regency, Maluku Province, Indonesia, *Journal of Geoscience, Engineering, Environment, and Technology*, Vol. 8, No. 4, 269–274. doi:10.25299/jgeet.2023.8.4.13788.
2. Montanaro, C., Ray, L., Cronin, S. J., Calibugan, A., Rott, S., Bardsley, C., and Scheu, B. (2023). Linking Top and Subsoil Types, Alteration and Degassing Processes at Rotokawa Geothermal Field, New Zealand, *Frontiers in Earth Science*, Vol. 10, No. January, 1–27. doi:10.3389/feart.2022.1067012.
3. Balali-Mood, M., Naseri, K., Tahergorabi, Z., Khazdair, M. R., and Sadeghi, M. (2021). Toxic Mechanisms of Five Heavy Metals: Mercury, Lead, Chromium, Cadmium, and Arsenic, *Frontiers in Pharmacology*, Vol. 12. doi:10.3389/fphar.2021.643972.
4. Pan, F., Huang, J., and Feng, X. (2024). Sources, Fates, and Geochemical Cycling of Mercury in Geothermal Fields: Insights From Mercury Isotopes, *Geophysical Research Letters*, Vol. 51, No. 9, 1–10. doi:10.1029/2023GL107384.
5. Liu, Q., Zheng, K., Wang, S., Wang, L., Lin, S., and Li, H. (2022). Arsenopyrite Oxidative Dissolution in NaCl Solution at High-Temperature and High-Pressure Conditions: Kinetics, Pathways, Dissolution Mechanism and Geological Implications, *Contributions to Mineralogy and Petrology*, Vol. 177, No. 7, 66. doi:10.1007/s00410-022-01929-2.
6. Hu, Y., Li, J., Lou, B., Wu, R., Wang, G., Lu, C., Wang, H., Pi, J., and Xu, Y. (2020). The Role of Reactive Oxygen Species in Arsenic Toxicity, *Biomolecules*, Vol. 10, No. 2, 240. doi:10.3390/biom10020240.
7. Charkiewicz, A. E., Omeljaniuk, W. J., Garley, M., and Nikliński, J. (2025). Mercury Exposure and Health Effects: What Do We Really Know?, *International Journal of Molecular Sciences*, Vol. 26, No. 5, 2326. doi:10.3390/ijms26052326.
8. Wu, Y.-S., Osman, A. I., Hosny, M., Elgarahy, A. M., Eltaweil, A. S., Rooney, D. W., Chen, Z., Rahim, N. S., Sekar, M., Gopinath, S. C. B., Mat Rani, N. N. I., Batumalaie, K., and Yap, P.-S. (2024). The Toxicity of Mercury and Its Chemical Compounds: Molecular Mechanisms and Environmental and Human Health Implications: A Comprehensive Review, *ACS Omega*, Vol. 9, No. 5, 5100–5126. doi:10.1021/acsomega.3c07047.
9. Yusnita, R. (2023). *Estimasi Karbon Serasah di Kawasan Manifestasi Geotermal Jaboi Kecamatan Sukajaya Kota Sabang.* UIN AR-Raniry Banda Aceh.
10. Idroes, R., Marwan, M., Yusuf, M., Muslem, M., and Helwani, Z. (2021). Geochemical Investigation on Jaboi Manifestation, Jaboi Volcano, Sabang, Indonesia, *International Journal of GEOMATE*, Vol. 20, No. 82. doi:10.21660/2021.82.j2114.
11. Afifah, N. A., and Notodarmojo, D. S. (2018). Identifikasi Sebaran Logam Berat Arsen (As) Dari Sistem Panas Bumi Pada Air Tanah Dangkal Dengan Metode Kriging, *Jurnal Teknik Lingkungan*, Vol. 24, No. April, 47–56.
12. Yuliyanti, A., Setiawan, I., Permana, H., Nurohman, H., Kausar, A. Al, Lintjewas, L., and Jakah, J. (2023). Environmental Study of the Potentially Harmful Elements (PHEs) in Talaga Bodas Geothermal Field, Indonesia, *AIP Conference Proceedings* (Vol. 2734), 040003. doi:10.1063/5.0155609.
13. Irnawati, I., Idroes, R., Zulfiani, U., Akmal, M., Suhartono, E., Idroes, G. M., Muslem, M., Lala, A., Yusuf, M., Saiful, S., Suhud, K., Safitri, E., and Jalil, Z. (2021). Assessment of Arsenic Levels in Water, Sediment, and Human Hair around Ie Seu'um Geothermal Manifestation Area, Aceh, Indonesia, *Water (Switzerland)*, Vol. 13, No. 17, 1–13. doi:10.3390/w13172343.
14. Idroes, R., Yusuf, M., Saiful, S., Alatas, M., Subhan, S., Lala, A., Muslem, M., Suhendra, R., Idroes, G. M., Marwan, M., and Mahlia, T. M. I. (2019). Geochemistry Exploration and Geothermometry Application in the North Zone of Seulawah Agam, Aceh Besar District, Indonesia, *Energies*, Vol. 12, No. 23, 4442. doi:10.3390/en12234442.
15. Lala, A., Yusuf, M., Suhendra, R., Maulydia, N. B., Dharma, D. B., Saiful, S., and Idroes, R. (2024). Characterization of Geochemical and Isotopic Profiles in the Southern Zone Geothermal Systems of Mount Seulawah Agam, Aceh Province, Indonesia, *Leuser Journal of Environmental Studies*, Vol. 2, No. 1, 30–40. doi:10.60084/ljes.v2i1.172.
16. Mabuat, J. C., Maddusa, S. S., Boky, H., Kesehatan, F., Universitas, M., and Ratulangi, S. (2017). Analisis Kandungan Logam Berat Timbal Pada Air, Ikan, Kerang Dan Sedimen Di Aliran Sungai Tondano Tahun 2017, *Kesmas*, Vol. 6, No. 3, 1–11.
17. Nasir, M., Sulastri, S., and Hilda, M. M. (2019). Analisis Kadar Logam Timbal Dan Arsenik Dalam Tanah Dengan Spektrometri Serapan Atom, *Jurnal IPA & Pembelajaran IPA*, Vol. 2, No. 2, 89–99. doi:10.24815/jipi.v2i2.12350.
18. Hindayani, A., and Hamim, N. (2022). Akurasi Dan Presisi Metode Sekunder Pengukuran Konduktivitas Menggunakan Sel Jones Tipe E Untuk Pemantauan Kualitas Air Minum, *IJCA (Indonesian Journal of Chemical Analysis)*, Vol. 5, No. 1, 41–51. doi:10.20885/ijca.vol5.iss1.art5.
19. Juliasih, N. L. G. R., Hidayat, D., Pirdaus, P., and Rinawati, R. (2021). Verification of the Determination Method of Dissolved Metal Content Using ICP-OES and Its Application for River Water in Bandar Lampung City, *Jurnal Kimia Sains Dan Aplikasi*, Vol. 24, No. 1, 29–36. doi:10.14710/jksa.24.1.29-36.

20. Akib Jabed, M., Paul, A., and Nath, T. K. (2020). Peoples' Perception of the Water Salinity Impacts on Human Health: A Case Study in South-Eastern Coastal Region of Bangladesh, *Exposure and Health*, Vol. 12, No. 1, 41–50. doi:10.1007/s12403-018-0283-0.

21. Durowoju, O. S., Ekosse, G.-I. E., and Odiyo, J. O. (2020). Occurrence and Health-Risk Assessment of Trace Metals in Geothermal Springs within Soutpansberg, Limpopo Province, South Africa, *International Journal of Environmental Research and Public Health*, Vol. 17, No. 12, 4438. doi:10.3390/ijerph17124438.

22. Brunetti B, D. E. (2015). About Estimating the Limit of Detection by the Signal to Noise Approach, *Pharmaceutica Analytica Acta*, Vol. 06, No. 04. doi:10.4172/2153-2435.1000355.

23. Fatmawati, F., Sunartaty, R., and Meutia, F. (2023). Validasi Metode Pengujian Kadar Air Dengan Analisis Perbandingan Akurasi Dan Presisi, *Serambi Journal of Agricultural Technology*, Vol. 5, No. 1, 59–63. doi:10.32672/sjat.v5i1.6214.

24. Prakash, S., and Verma, A. K. (2021). Arsenic: It's Toxicity and Impact on Human Health, *International Journal of Biological Innovations*, Vol. 03, No. 01, 38–47. doi:10.46505/IJBI.2021.3102.

25. Rauf, A. U., Mallongi, A., And Astuti, R. D. P. (2020). Mercury and Chromium Distribution in Soil Near Maros Karst Ecosystem, *Carpathian Journal of Earth and Environmental Sciences*, Vol. 15, No. 2, 453–460. doi:10.26471/cjees/2020/015/144.

26. Long, E. R., and Macdonald, D. D. (2010). Recommended Uses of Empirically Derived , Sediment Quality Guidelines for Marine and Estuarine Ecosystems PERSPECTIVE : Recommended Uses of Empirically Derived , Sediment Quality Guidelines for Marine And, *Human and Ecological Risk Assessment: An International Journal*, No. October 2012, 37–41.

27. Knappett, P. S. K., Li, Y., Loza, I., Hernandez, H., Avilés, M., Haaf, D., Majumder, S., Huang, Y., Lynch, B., Piña, V., Wang, J., Winkel, L., Mahlknecht, J., Datta, S., Thurston, W., Terrell, D., and Kirk Nordstrom, D. (2020). Rising Arsenic Concentrations from Dewatering a Geothermally Influenced Aquifer in Central Mexico, *Water Research*, Vol. 185, 116257. doi:10.1016/j.watres.2020.116257.

28. Ewers, G. R., and Keays, R. R. (1977). Volatile and Precious Metal Zoning in the Broadlands Geothermal Field, New Zealand, *Economic Geology*, Vol. 72, No. 7, 1337–1354. doi:10.2113/gsecongeo.72.7.1337.